Carbohydrate Polymers 86 (2011) 453–461

Contents lists available at ScienceDirect

Carbohydrate Polymers

journal homepage: www.elsevier.com/locate/carbpol

Preparation of millimeter-long cellulose I nanofibers with diameters of 30–80 nm from bamboo fibers

Wenshuai Chen, Haipeng Yu*, Yixing Liu

Key Laboratory of Bio-based Material Science and Technology, Ministry of Education, Northeast Forestry University, Harbin 150040, China

ARTICLE INFO

Article history:
Received 2 April 2011
Accepted 24 April 2011
Available online 1 May 2011

Keywords:
Ultralong
Cellulose nanofibers
Bamboo
Chemical treatment
Ultrasonic treatment

ABSTRACT

Ultralong and highly uniform cellulose I nanofibers (CNFs) with lengths >1 mm, diameters of 30–80 nm, and aspect ratios >10,000 were successfully prepared from bamboo fibers, by using chemical pretreatment combined with high intensity ultrasonication to purify and defibrillate bamboo fibers into parallel arrays cellulose nanofibrils (1–5 nm width and several microns long), and then assembling the nanofibrils into ultralong CNFs by simple freeze-drying; Similar findings were also observed from the micrographs of CNFs fabricated from wheat straw and softwood fibers. The chemical composition of the fabricated CNFs is mainly cellulose because hemicelluloses and lignin were appreciably removed during the chemical process. With the removal of the matrix materials, the cellulose I crystal structure was maintained, whereas the crystallinity and thermal stability of the fibers increased. The crystallinity and thermal degradation temperature of the CNFs reached 61.25% and over 309 °C, respectively. Ultralong CNFs could serve as unique building blocks for green nanocomposites and are expected to open up new opportunities for application in tissue engineering scaffolds.

1. Introduction

Cellulose is the most abundant biopolymer on earth and is present in accounts for approximately 40% of plant biomass. It is a long-chain polysaccharide composed of β-1,4-linked D-glucose rings with polymer chains associated by both hydrogen bonds and van der Waals forces forming fibrous structures called microfibrils. The microfibrils are a few nanometers across having highly ordered regions (i.e., crystalline phases) alternating with disordered domains (i.e., amorphous phases) (Klemm, Heublein, Fink, & Bohn, 2005). The crystalline regions of the microfibrils consist of stiff, close-packed extended cellulose chains with strong intermolecular forces that result in Young's Modulus values exceeding 100 GPa (Sakurada, Nukushina, & Ito, 1962) as well as negligible thermal expansion (Bergenstråhle, Berglund, & Mazeau, 2007; Nishino, Matsuda, & Hirao, 2004) in the chain direction. When the cellulose microfibrils and related nanofibers are isolated from the plant fibers or other natural polysaccharides such as chitin (Fan, Saito, & Isogai, 2008; Ifuku et al., 2009), functionalities such as biodegradability, reproducibility, and biocompatibility are also introduced to the nanofibers. These features make cellulose nanofibers (CNFs) prospective nanoelements in the field of materials sciences (Beecher, 2007; Capadona et al., 2007; Dong & Roman, 2007; Shopsowitz, Qi, Hamad, & MacLachlan, 2010).

Numerous fabrication methods for isolating CNFs from various plant fibers have been attempted (for recent reviews, see Azizi Samir, Alloin, & Dufresne, 2005; Berglund, 2005; Eichhorn et al., 2010; Habibi, Lucia, & Rojas, 2010; Siró & Plackett, 2010); notable examples include those based on mechanical treatments, e.g., cryocrushing (Chakraborty, Sain, & Kortschot, 2005; Chakraborty, Sain, & Kortschot, 2006), grinding (Abe, Iwamoto, & Yano, 2007; Abe & Yano, 2009; Iwamoto, Abe, & Yano, 2008), high-pressure homogenizing (Herrick, Casebier, & Hamilton, 1983; Turbak, Snyder, & Sandberg, 1983), and high-speed blendering (Uetani & Yano, 2011); chemical treatments, e.g., sulfuric acid hydrolysis (Beck-Candanedo, Roman, & Gray, 2005; Elazzouzi-Hafraoui et al., 2007; Marchessault, Morehead, & Walter, 1959) and hydrochloric acid hydrolysis (Araki, Wada, Kuga, & Okano, 1998); biological treatments, e.g., enzyme-assisted hydrolysis (Henriksson, Henriksson, Berglund, & Lindstrom, 2007; Pääkkö et al., 2007, 2008); TEMPO-mediated oxidation (Isogai, Saito, & Fukuzumi, 2011; Saito, Kimura, Nishiyama, & Isogai, 2007); as well as a combination of two or several of these methods. All these methods lead to different types of nanofibrillar materials, depending on the starting material and pretreatment, and more importantly, depending upon the disintegration process itself.

CNFs individualized by the aforementioned methods, termed as cellulose nanocrystals, whiskers, nanowhiskers, microfibril-

* Corresponding author at: College of Material Science and Engineering, Northeast Forestry University, No. 26 Hexing Road, Xiangfang District, Harbin 150040, China. Tel.: +86 451 8219 1756; fax: +86 451 8219 0134.
E-mail address: yuhaipeng20000@yahoo.com.cn (H. Yu).

0144-8617/$ – see front matter © 2011 Elsevier Ltd. All rights reserved.
doi:10.1016/j.carbpol.2011.04.061

lated cellulose, microfibril aggregates, nanofibers, have found widespread use as reinforced nanocomposites, foams, aerogels, (Siqueira, Bras, & Dufresne, 2008; Svagan, Samir, & Berglund, 2008), optically transparent functional materials (Nogi, Iwamoto, Nakagaito, & Yano, 2009; Sehaqui, Liu, Zhou, & Berglund, 2010), and oxygen-barrier layers (Fukuzumi, Saito, Iwata, Kumamoto, & Isogai, 2009); despite this, their lengths are often limited to the micron scale or are less than 100 nm due to aggressive hydrolysis or high shearing forces which attack the noncrystalline fractions during fibrillation. However, in some specific applications such as tissue engineering scaffolds, ultralong CNFs are needed to mimic the architecture of the extracellular matrix (ECM) for cell attachment and nutrient transportation (Xia, 2008; Xie, Li, & Xia, 2008). In addition, ultralong CNFs have a high aspect ratio and surface area as well as a web-like entangled structure which could improve the toughening of the composites, all of which may provide new opportunities for many applications. Thus, the preparation of highly uniform and ultralong CNFs from plant fibers is a very important and challenging issue. Compared with the conventional top-down process, electrospinning seems better-suited for generating fibers of high length and uniform width (Li & Xia, 2004). However, the dissolution process prior to electrospinning often leads to the structural elements of the amorphous or cellulose II type (Kim, Kim, Kang, Marquez, & Joo, 2006), which typically has reduced strength.

To extract ultralong CNFs with cellulose I crystal form from natural plant fibers, initial chemical treatment is required to fabricate highly purified cellulose I fibers. Furthermore, rational fibrillation is important for the disintegration of chemically purified fibers into slender nanofibers. Among all CNFs preparation routes, ultrasonication seems to be a well method suited for isolating CNFs with relatively high lengths (Cheng, Wang, Rials, & Lee, 2007; Cheng, Wang, & Rials, 2009; Tischer, Sierakowski, Westfahl, & Tischer, 2010; Zhao, Feng, & Gao, 2007). Because this fibrillation method mainly relies on the effect of acoustic cavitation of high frequency ultrasound in the formation, expansion, and implosion of microbubbles in aqueous solution. The violent collapse induces microjets and shock waves on the surface of the purified cellulose fibers, causing erosion which leads to a split along the axial direction. The sonification impact can break the relatively weak interfaces between the microfibrils bonded mainly by nonbonding interactions such as van der Waals forces (Zhao et al., 2007). On the other hand, the covalent bonds along the longitudinal direction of the cellulose molecule chains remain intact (Li & Renneckar, 2011). Ultrasonication therefore has potential to extract and maintain the original lengths of the microfibrils. However, microfibrils in plant cell walls are only several microns in length (Burgess, 1979) and ~3 nm in width (Somerville et al., 2004). The lengths of CNFs obtained by ultrasonication will therefore hardly to reach 100 μm. It is therefore necessary to choose an efficient method to assemble the micron-long fibrils into millimeter-long CNFs.

A route proposed here is to prepare millimeter-scale CNFs of uniform diameters and of the cellulose I crystal form from bamboo fibers. Highly purified cellulose fibers were first produced by chemical pretreatment. Next, high intensity ultrasonication was conducted to isolate slender nanofibrils (as the obtained samples were 1–5 nm width and several microns long, so a term of cellulose nanofibrils was used here compared with that of millimeter-long CNFs) and to disperse them in water. The resulting cellulose nanofibrils were further assembled into millimeter-long CNFs by a freeze-drying method. The chemical composition, morphology, crystalline behavior, and thermal property of the CNFs and their intermediate products were characterized and compared in detail by means of chemical analysis, field emission scanning electron microscope (FE-SEM), transmission electron microscope (TEM), Fourier transform infrared spectroscopy (FTIR), X-ray diffraction (XRD), and thermogravimetric analysis (TG).

2. Experimental

2.1. Raw materials

Bamboo, wheat straw, and softwood fibers were used as native cellulose fibers. Mature culms of Moso bamboo were collected from Zhejiang Province, China. Wheat straw and softwood (from *Abies nephrolepis*) fibers were collected from local farms in Heilongjiang Province, China in 2007. All samples sieved under 60 mesh were air-dried and stored at room temperature. Benzene, ethanol, sodium chlorite, acetic acid, potassium hydroxide, hydrochloric acid, and other chemicals were of laboratory grade and were used without further purification.

2.2. Removal of matrix components

Chemical purification of bamboo, wheat straw and softwood fibers was performed according to literature with minor modifications (Chen et al., 2011). Briefly, 2 g of samples was dewaxed in a Soxhlet apparatus with a 2:1 (v/v) mixture of benzene/ethanol for 6 h. Afterward, lignin in the samples was removed using an acidified sodium chlorite solution at 75 °C for an hour; the process was repeated five times, resulting in holocellulose fibers (Ho-CFs). Next, the Ho-CFs were treated with 2 wt% potassium hydroxide at 90 °C for 2 h to remove hemicelluloses, residual starch, and pectin. To obtain highly purified cellulose, the samples were further treated with an acidified sodium chlorite solution at 75 °C for an hour and then treated with 5 wt% potassium hydroxide at 90 °C for 2 h, resulting in alkali-treated cellulose fibers (Al-CFs). Last, highly purified acid-treated cellulose fibers (Ac-CFs) were prepared by treating Al-CFs with 1 wt% hydrochloric acid solution at 80 °C for 2 h and thoroughly washing them with distilled water. To avoid generating strong hydrogen bonds between the cellulose bundles after matrix components removal, the samples were kept in the water-swollen state all the time. Nomenclatures for the different kinds of cellulose fibers are: Raw-BFs, raw bamboo fibers; Ho-CFs, holocellulose fibers; Al-CFs, alkali-treated cellulose fibers; and Ac-CFs, acid-treated cellulose fibers.

2.3. Ultrasonical disintegration

After chemical pretreatment, highly purified Ac-CFs were soaked in distilled water at approximately 0.05% (w/w) solid content. About 120 ml of a solution containing Ac-CFs was then placed in a common ultrasonic generator (JY98-IIID, Ningbo Scientz Biotechnology Co., Ltd., China) 20–25 kHz in frequency and equipped with a cylindrical titanium alloy probe tip 1.5 cm in diameter. The subsequent ultrasonication was conducted for 30 min at an output power of 1200 W, resulting in a cellulose nanofibrils suspension. The sonicated suspension was then centrifuged to separate the large bundles from the nanofibrils; slender nanofibrils were obtained from the supernatant fraction. The bundles of the nanofibrils, collected as sediments, were re-treated by high intensity ultrasonication. Ultrasonic treatment was carried out in an ice/water bath. Ice was maintained throughout the entire ultrasonication.

2.4. Assembly of the cellulose nanofibrils into ultralong CNFs

The transparent supernatant of the cellulose nanofibrils obtained after centrifugation was poured into a glass Petri dish (the thickness of water "layer" is about 2 mm) and then placed in a refrigerator at −18 °C for more than 24 h. The sample was then placed in a freeze-dryer (Scientz-10N, Ningbo Scientz Biotechnology Co., Ltd, China) to allow frozen water in the material to sublime directly from the solid phase to the gas phase, and to assemble the cellulose nanofibrils into ultralong CNFs owing to the driving forces

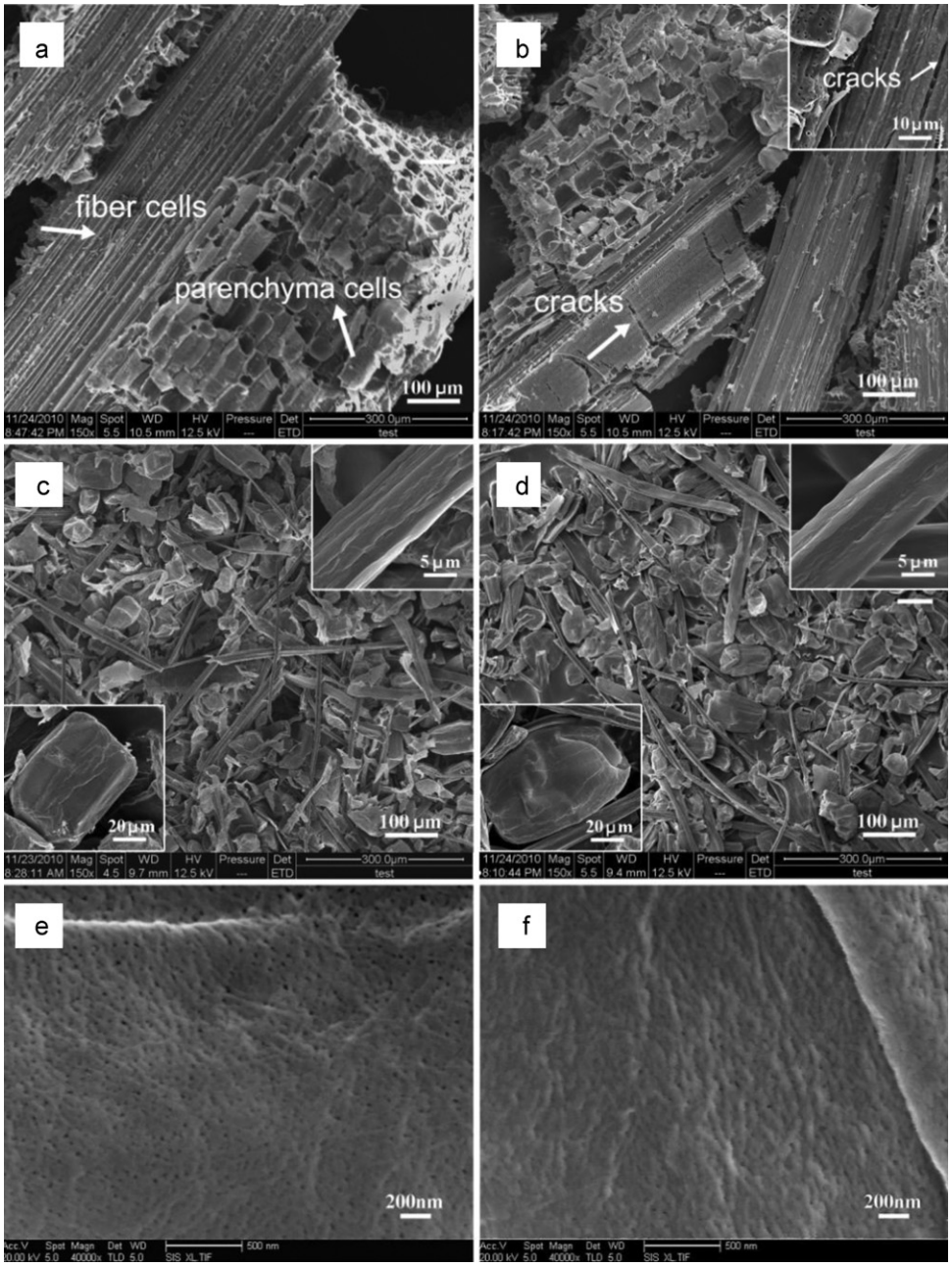

Fig. 1. SEM images of (a) Raw-BFs, (b) Ho-CFs (insert shows the high magnification SEM graph of Ho-CFs), (c) Al-CFs (insert shows SEM graphs of single fiber and parenchyma cell of Al-CFs, respectively), (d) Ac-CFs (insert shows SEM graphs of single fiber and parenchyma cell of Ac-CFs, respectively), and FE-SEM micrographs of the surface of fiber (e) and parenchyma (f) cells of (d).

of hydrogen bonds formed between the hydroxyl groups of cellulose. The cold trap temperature was <−55 °C and the vacuum was <15 Pa during the freeze-drying process.

2.5. Chemical composition measurement

The chemical composition of the untreated and chemically treated bamboo fibers was measured in accordance with the standards of the Technical Association of Pulp and Paper Industry (TAPPI). The holocellulose (cellulose + hemicelluloses) content was determined according to the method described in TAPPI T19m-54. The α-cellulose content of the fibers was then determined by further NaOH treatment of the fibers to remove the hemicelluloses. The difference between the values of holocellulose and α-cellulose gives the hemicelluloses content of the fibers. Lignin content was analyzed by reaction with sulfuric acid using the standard method recommended in TAPPI-T222 om-88. A minimum of three samples from each material was tested, and the averaged values were obtained.

2.6. Optical transmittance

A cellulose nanofibrils dispersion was introduced into a poly(methyl methacrylate) disposable cuvette, and the transmittance was measured from 300 to 800 nm using a UV–vis spectrophotometer (TU-1900, Beijing Purkinje General Instrument Co., Ltd., China). The spectrum of a cuvette filled with water was used as a reference to correct the transmittance of the dispersion.

2.7. Transmission electron microscope (TEM)

Transmission electron microscope (TEM) images of the cellulose nanofibrils were taken using a FEI Tecnai G2 electron microscope at 80 kV acceleration voltage. Drops of dilute nanofibrils suspensions were deposited onto glow-discharged, carbon-coated, electron microscopy grids; excess liquid was absorbed by a piece of filter paper. The samples were subsequently stained with a 2% phosphotungstic acid solution to enhance microscopic resolution. Diameters of the cellulose nanofibrils were calculated from the TEM images using a microscope image analysis system (TDY-V5.2, Beijing Tianhong Precision Instrument Technology Co., Ltd., China), which were used to illustrate size distributions.

2.8. Scanning electron microscope (SEM)

Suspensions of the cellulose fibers before and after the ultrasonic process were subjected to freeze-drying; the obtained sheets were coated with gold by an ion sputter coater and were observed through scanning electron microscope (Quanta200, FEI, USA) and through field emission scanning electron microscope (Sirion 200, FEI, Netherlands). Diameters of the CNFs were calculated from FE-SEM images using a microscope image analysis system (TDY-V5.2, Beijing Tianhong Precision Instrument Technology Co., Ltd., China), which were used to illustrate size distributions.

2.9. FT-IR spectroscopy

FTIR spectra were recorded on a Fourier Transform Infrared Instrument (Magna 560, Nicolet, Thermo Electron Corp., USA) in the range of 400–4000 cm^{-1} with a resolution of 4 cm^{-1}. The dried samples were ground into powder by a fiber microtome and were then blended with KBr before being pressed into ultra-thin pellets.

2.10. X-ray diffraction analysis

The XRD patterns for Raw-BFs, chemically treated cellulose fibers, and isolated CNFs were measured with an X-ray diffractometer (D/max 2200, Rigaku, Japan) using Ni-filtered Cu Kα radiation (λ = 1.5406 Å) at 40 kV and 30 mA. Scattered radiation was detected in the range of $2\theta = 5–40^\circ$ at a scan rate of 1°/min. The crystallinity index (*CI*) was calculated from the height of the 200 peak (I_{200}, $2\theta = 22.6^\circ$) and the intensity minimum between the peaks at 200 and 110 (I_{am}, $2\theta = 18^\circ$) using the Segal method (Segal, Creely, Martin, & Conrad, 1959) (Eq. (1)). I_{200} represents both a crystalline and amorphous material, whereas I_{am} represents an amorphous material.

$$CI\ (\%) = \left(1 - \frac{I_{am}}{I_{200}}\right) \times 100 \quad (1)$$

2.11. Thermal stability

Thermogravimetric analysis was performed to compare the degradation characteristics of Raw-BFs, chemically treated cellulose fibers, and isolated CNFs. The thermal stability of each sample was determined using a thermogravimetric analyzer (Pyris 6, PerkinElmer, USA) at a heating rate of 10 °C/min in a nitrogen environment.

3. Results and discussion

3.1. Preparation of chemically purified cellulose fibers

To extract highly purified cellulose fibers from Raw-BFs, hemicelluloses and lignin were removed according to conventional methods using $NaClO_2$ and KOH solutions, respectively. HCl treatment was conducted to remove the alkali insoluble matrix components. The changes in chemical composition due to chemical treatment are presented in Table 1. Raw-BFs have the highest percentage of hemicelluloses (27.2%) and lignin (23.2%) and the lowest percentage of α-cellulose (41.8%). When the fibers were subjected to $NaClO_2$ treatment, the lignin concentration of the Ho-CFs decreased to 0.1%, whereas the α-cellulose and hemicelluloses concentration of the Ho-CFs increased to 64.7% and 35.3%, respectively. After KOH treatment, the α-cellulose concentration of the Al-CFs increased to 84.4% due to the hydrolyzation of the hemicelluloses. When HCL treatment was conducted, the α-cellulose concentration of the Ac-CFs further increased to 93.3%, resulting in highly purified cellulose fibers.

Table 1
Chemical compositions of Raw-BFs, Ho-CFs, Al-CFs and Ac-CFs.

Samples	α-Cellulose (%)	Hemicelluloses (%)	Total lignin (%)
Raw-BFs	41.8 ± 1.9	27.2 ± 4.3	23.2 ± 2.7
Ho-CFs	64.7 ± 0.7	35.3 ± 4.5	0.1
Al-CFs	84.4 ± 1.8	14.6 ± 1.5	0.1
Ac-CFs	93.3 ± 2.7	6.7 ± 2.5	0.1

The cellulose fiber structure changed according to the removal of matrix components (Fig. 1). The Raw-BFs are composed of fiber cells and parenchyma cells (Fig. 1a); the structures of both were also maintained after $NaClO_2$ treatment removed most of the lignin (Fig. 1b). However, cracks are frequently observed in the Ho-CFs, indicating that cohesion between the fibers was reduced. When KOH treatment was performed to hydrolyze most hemicelluloses, a number of single cells were obtained (Fig. 1c). The single cells were clearly distinguished into two different types: fibrous cells and rectangular cells (regarded mostly as fiber and parenchyma cells, respectively). After HCl treatment, the microstructure of both cells was maintained and single fibrous cells as well as parenchyma cells can be clearly observed (Fig. 1d). High magnification FE-SEM micrographs (Fig. 1e and f) show a similar appearance of continuous nanofibrils having widths smaller than 20 nm in both cells. These micrographs are in excellent agreement with previous research (Abe & Yano, 2010). To extract these nanofibrils from the purified Ac-CFs, an efficient defibrillation process is required.

3.2. Ultrasonication of Ac-CFs in water

The chemically purified Ac-CFs were subjected to ultrasonic treatment. Photographs of the dispersions of the obtained cellu-

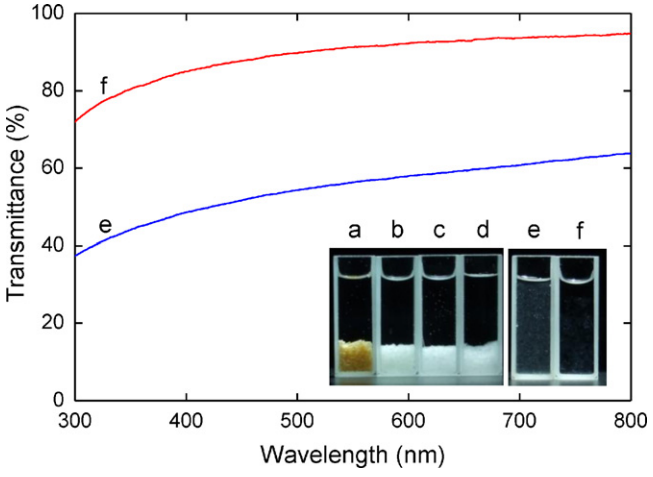

Fig. 2. Photographs of dispersions of (a) Raw-BFs, (b) Ho-CFs, (c) Al-CFs, (d) Ac-CFs, (e) 0.05 wt% cellulose nanofibrils after ultrasonication, and (f) supernatant of suspension e after centrifugation at 6000 r/min for 5 min, the concentration was carefully adjusted to 0.05 wt% by evaporation of the water.

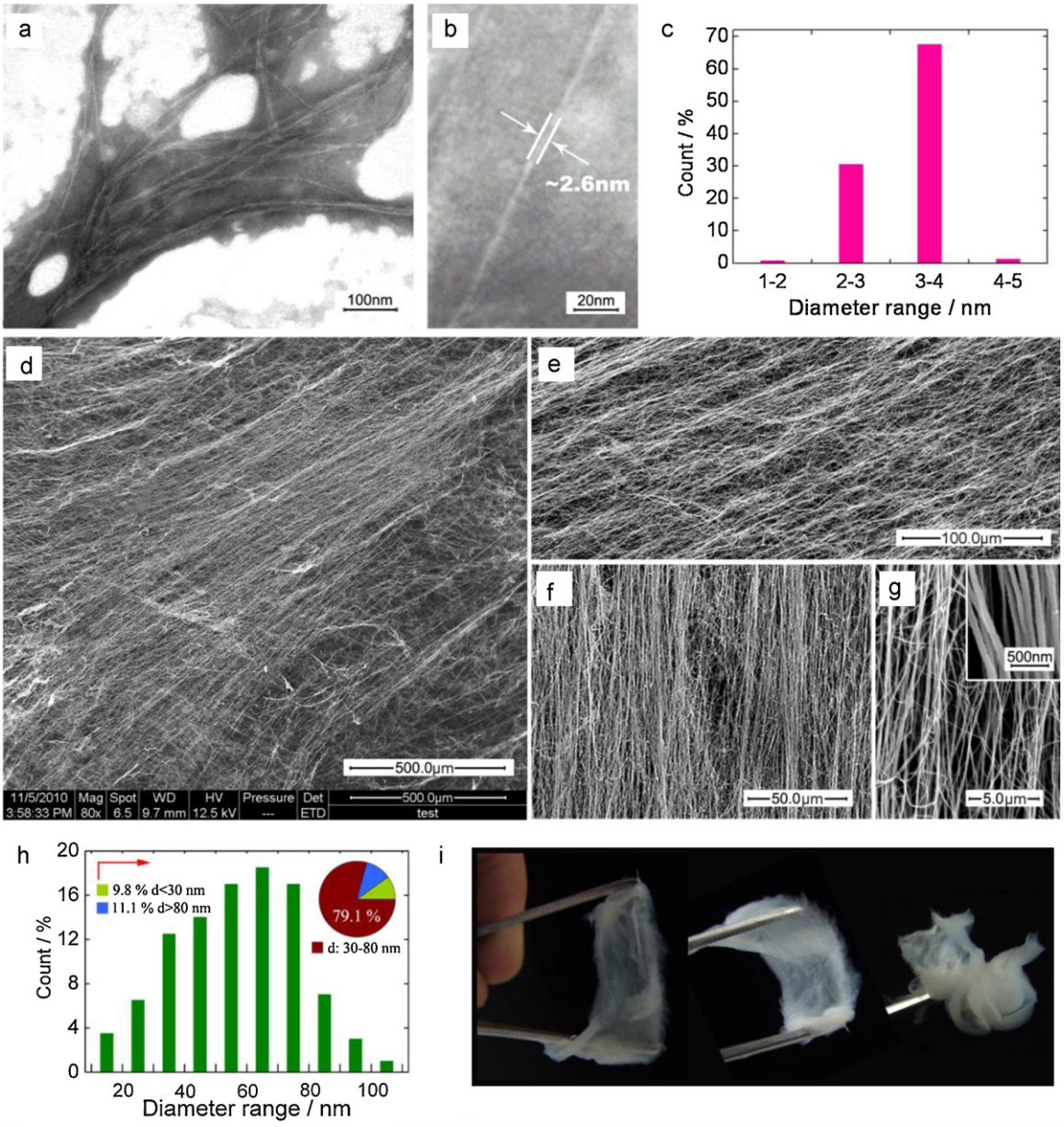

Fig. 3. Assemble of the bamboo cellulose nanofibrils into ultralong CNFs.

lose nanofibrils and their intermediate products in water, and of the corresponding visible-light transmittances are shown in Fig. 2. Raw-BFs sediment spontaneously at the bottom of the glass bottle and yellow fibers became white after $NaClO_2$ treatment, indicating that an appreciable amount of lignin was removed. The fiber shape of the Ho-CFs in water was maintained after KOH and HCL treatment; all fibers precipitated at the bottom of the glass bottle leaving no dispersion in water. When 1200 W ultrasonication of the Ac-CFs was conducted for 30 min, the obtained nanofibrils dispersed in water (Fig. 2e). However, the dispersion had high turbidity. The transmittance of 0.05 wt% suspension at 600 nm was <60%, indicating that an appreciable amount of bundles or aggregates of the nanofibrils were still present in the dispersion. Therefore, fibers that were not completely disintegrated into nanofibrils were separated as sediments by centrifugation and highly transparent cellulose nanofibrils dispersion was obtained from the supernatant fraction (Fig. 2f). The transmittance of the dispersion was over 85% for visible light. The slurry of the cellulose nanofibrils exhibited remarkably high viscosity. The cellulose nanofibrils/water dispersion at 0.3 wt% consistency formed hard gels and was converted into an optically transparent film after oven drying (Figure S1 in Supporting Information). A homogeneous dispersion of cellulose nanofibrils with high surface-to-volume ratio in water was therefore obtained.

3.3. Assembly of the cellulose nanofibrils into ultralong CNFs

TEM observations (Fig. 3a and b) reveal that high intensity ultrasonication resulted in the defibrillation of Ac-CFs into slender cellulose nanofibrils having 1–5 nm cross-sectional width (Fig. 3c) and at least a few microns long. The nanofibrils were ordered along the longitudinal direction and some aggregates were also observed (Figure S2 in Supporting Information). The appearance of laterally aggregated nanofibrils in the TEM images is expected due to the high specific area and strong hydrogen bonds established between the nanofibrils. When the dispersing aqueous medium was slowly removed by freeze-drying, the nanofibrils and their aggregates were assembled parallel to each other and were aligned side-by-

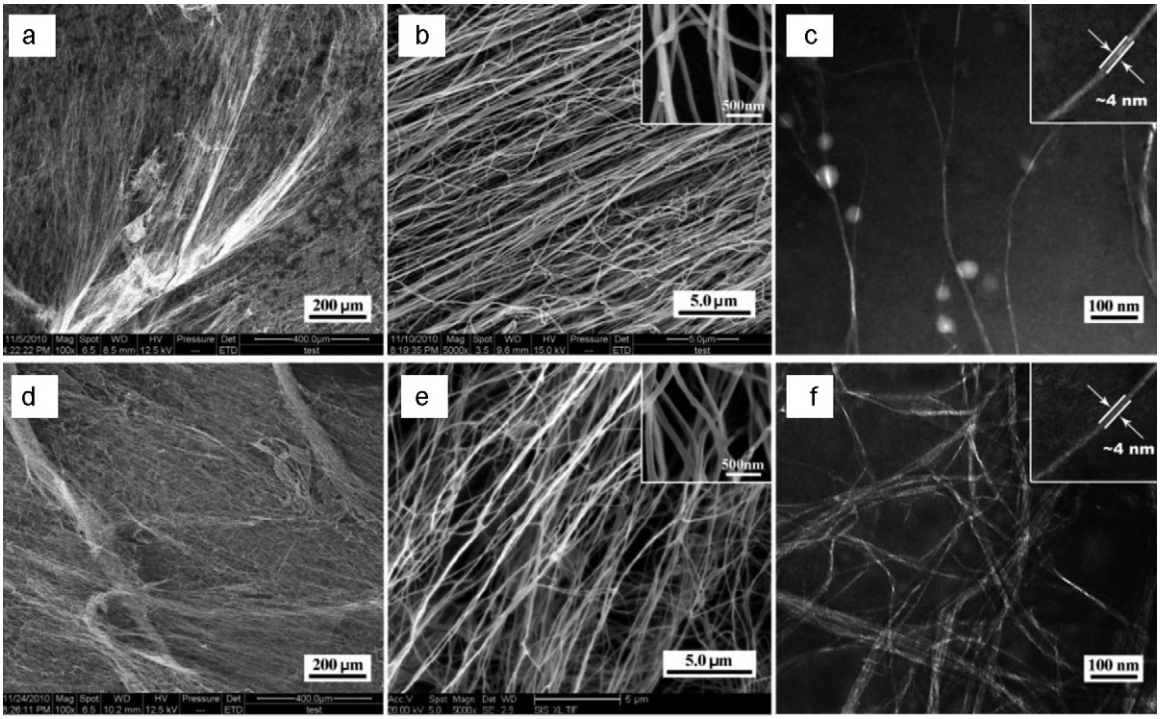

Fig. 4. Structural characterization of ultralong CNFs produced from wheat straw and softwood (from *Abies nephrolepis*) fibers. (a) SEM image of wheat straw CNFs; (b) FE-SEM image of wheat straw CNFs (insert shows the high magnification FE-SEM graph of wheat straw CNFs); (c) TEM image of wheat straw cellulose nanofibrils (insert shows TEM image of single wheat straw cellulose nanofibril). (d) SEM image of softwood (from *Abies nephrolepis*) CNFs; (e) FE-SEM image of softwood (from *Abies nephrolepis*) CNFs (insert shows the high magnification FE-SEM graph of softwood (from Abies nephrolepis) CNFs); (f) TEM image of softwood (from *Abies nephrolepis*) cellulose nanofibrils (insert shows TEM image of single softwood (from *Abies nephrolepis*) cellulose nanofibril).

side by the driving forces of hydrogen bonds that formed between the hydroxyl groups on the surface of the cellulose nanofibrils, as well as the bonding energies contributed by other interactions, thus organizing them into ultralong CNFs without the use of binders. The low magnification SEM images (Fig. 3d and Figure S3 in Supporting Information) show that the lengths of these individual CNFs are larger than one millimeter. We even have found the longest cellulose nanofiber with a length at or exceeding 4 mm during our SEM observation, which is almost 2000 times longer than the nanowhiskers typically produced by acid hydrolysis methods (Siró & Plackett, 2010). The ultralong CNFs exhibited a very straight and smooth surface with uniform diameters; no defects were observed at the surface of the CNFs (Fig. 3d–g and Figure S4 in Supporting Information). The diameters of 79.1% of the CNFs range from 30 to 80 nm (Fig. 3h). The aspect ratio of single CNFs was over 10,000. As the TEM observation reveals that most of the slender cellulose nanofibrils were 1–5 nm in width and were several microns long. Thus, each millimeter-scale cellulose nanofiber consists of millions of slender nanofibrils along the longitudinal direction. Fig. 3i shows a CNFs sheet that is light, flexible, and can easily be handled by tweezers. Such a porous sheet consisting of ultralong CNFs, are expected to find use in various fundamental and applied fields such as self-assembled nanofiber templates for green nanocomposites, tissue engineering scaffolds, filtration media, and packaging films.

Ultralong CNFs were also individualized from other cellulosic materials using the same methods. For wheat straw (Fig. 4a and b, and Figure S5 in Supporting Information) and softwood (from *Abies nephrolepis*) (Fig. 4d and e, and Figure S6 in Supporting Information) fibers, SEM images confirm that millimeter-scale CNFs may also be successfully obtained as effectively as from bamboo fibers. The lengths of the CNFs were larger than 1 mm, the diameters range of the isolated CNFs from wheat straw and softwood fibers, was 50–100 nm (Figure S7 in Supporting Information) and 40–90 nm (Figure S8 in Supporting Information), respectively. Slender nanofibrils, 2–7 nm in diameters (Figures S9 and S10 in Supporting Information), were also observed from the TEM micrographs of the suspensions of wheat straw and softwood CNFs (Fig. 4c and f), indicating that the obtained ultralong CNFs were also assembled from slender cellulose nanofibrils during freeze-drying. Furthermore, ultralong CNFs were also produced from hardwood (from *Populus* spp.) and bagasse fibers (Figures S11 and S12 in Supporting Information). These results indicate that the simple method mentioned in this paper may also be extended to fabricate ultralong nanofibers from many other kinds of natural polysaccharides such as cellulose or chitin by carefully controlling the process conditions.

3.4. Chemical and crystal structures of CNFs

FT-IR spectra of the bamboo CNFs and their intermediate products are shown in Fig. 5. The peak at 1508 cm^{-1} in the spectrum of the Raw-BFs, which is attributed to the C=C stretching vibration in the aromatic ring of lignin, disappeared completely in the Ho-CFs. This indicates that lignin was well removed from the newly prepared Ho-CFs by $NaClO_2$ treatment. The peaks at 1737 cm^{-1} in the spectrum of the Ho-CFs represent either the acetyl and uronic ester groups or the ester linkage of carboxylic group of the ferulic and p-coumeric acids of hemicelluloses (Alemdar & Sain, 2008). The absence of this peak in the Al-CFs is attributed to the removal of most of the hemicelluloses during the KOH process. When HCl treatment was further conducted, the main absorbance peaks of the Ac-CFs were similar to that of the Al-CFs, indicating that only a small amount of alkali insoluble hemicelluloses and lignin remained and were removed by HCL. These results are in excellent agreement with the chemical composition analysis shown in Table 1. After ultrasonic fibrillation, the spectrum of the CNFs was fairly close to that of the Ac-CFs. The band at 3400 cm^{-1} is attributed to O–H stretching vibration. The bands at 2893 and 1431 cm^{-1} are characteristics of C–H stretching and the bending of

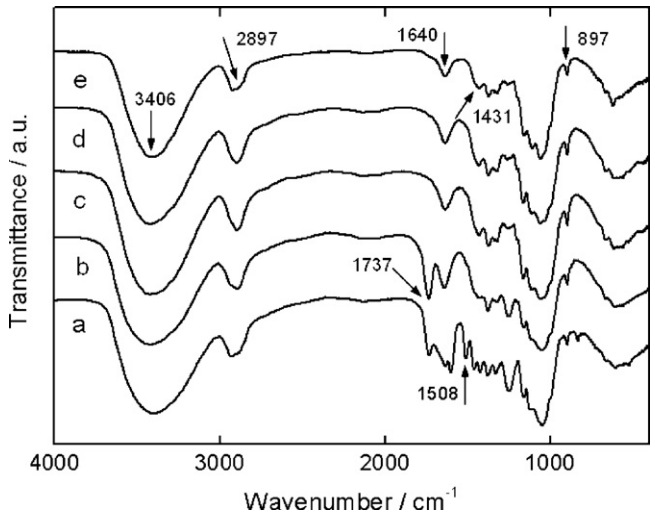

Fig. 5. FT-IR spectra of (a) Raw-BFs, (b) Ho-CFs, (c) Al-CFs, (d) Ac-CFs, and (e) CNFs.

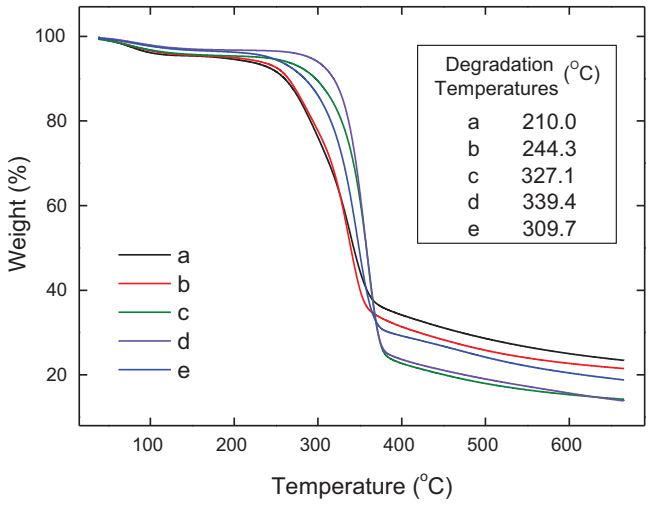

Fig. 7. TG curves and degradation temperatures (insert) of (a) Raw-BFs, (b) Ho-CFs, (c) Al-CFs, (d) Ac-CFs, and (e) CNFs.

$-CH_2$ groups, respectively, whereas the peaks at 1640 and 897 cm^{-1} are attributed to the H–O–H stretching vibration of absorbed water in carbohydrate and the C_1–H deformation vibrations of cellulose, respectively. This fact indicated that a larger amount of hemicelluloses and lignin were removed during the chemical procedures and the original molecular structure of cellulose was maintained even after matrix components removal and ultrasonic treatments.

Fig. 6 is a comparison of the X-ray diffraction profiles and the apparent crystallinity of the Raw-BFs, chemically treated cellulose fibers, and CNFs. All samples had diffraction peaks at $2\theta = 16.5^\circ$ and 22.5° and are believed to represent the typical cellulose I pattern (Nishiyama, Langan, & Chanzy, 2002; Nishiyama, Sugiyama, Chanzy, & Langan, 2003). Thus, the original cellulose crystal integrity was maintained during the process of CNFs preparation. However, the apparent crystallinity of the fibers apparently changed. The apparent crystallinity of the Raw-BFs was 53.39%. After $NaClO_2$ treatment, the apparent crystallinity of the Ho-CFs increased to 57.65% owing to the removal of lignin. The apparent crystallinity of the Al-CFs increased to 66.91% because of the removal of most hemicelluloses which exist in the amorphous regions. A slight decrease in crystallinity occurred upon HCL treatment. After ultrasonic defibrillation, the ultrasonic defibrillation of the CNFs decreased compared with that of the Ac-CFs, indicating that a substantial part of the noncrystalline domains remain essentially intact; this could lead to high length and aspect ratio of the CNFs. However, the apparent crystallinity of the CNFs was still as high as 61.25%. The high crystalline CNFs could be more effective in providing better reinforcement for composite materials because the high Young's modulus (138 GPa) of the crystal region along the longitudinal direction (Sakurada et al., 1962).

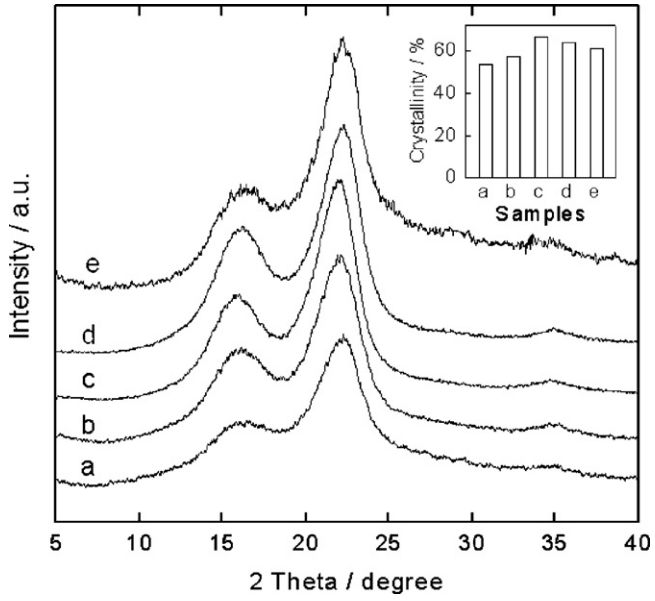

Fig. 6. X-ray diffraction patterns and crystallinities (insert) of (a) Raw-BFs, (b) Ho-CFs, (c) Al-CFs, (d) Ac-CFs, and (e) CNFs.

3.5. Thermal properties of the CNFs

Fig. 7 shows thermogravimetric curves of Raw-BFs, chemically treated cellulose fibers, and CNFs. All the TG curves show an initial small drop between 50 °C and 150 °C, which corresponds to a mass loss of approximately 5% absorbed moisture. Decomposition of the Raw-BFs shows several stages, indicating the presence of different components that decompose at different temperatures. Due to the low decomposition temperatures of hemicelluloses, lignin, and pectin, the Raw-BFs started to degrade at around 210.0 °C, and their dominant thermogravimetric (DTG) peak was observed at around 344.5 °C accounted for the pyrolysis of cellulose. The degradation temperature of Ho-CFs slightly increased to 244.3 °C due to the removal of lignin. After most of the hemicelluloses were hydrolyzed by the KOH treatment, the degradation temperature of the Al-CFs was apparently increased to 327.1 °C; this further increased to 339.4 °C when HCL treatment was conducted to remove the alkali insoluble matrix components. For the CNFs, degradation began at 309.7 °C. Thus, a substantial part of the noncrystalline domains existed after the ultrasonication and freeze-drying processes which are necessary for the preparation of ultralong CNFs. These results corroborate the results obtained from chemical composition analysis, FTIR, and X-ray measurement. The higher thermal stability of the CNFs relative to the Raw-BFs may broaden the application area of the cellulose fibers especially at the temperatures larger than 200 °C for biocomposite processing.

4. Conclusion

Ultralong CNFs of cellulose I crystal form, >1 mm in length, and 30–80 nm in diameter were prepared from bamboo fibers by conventional chemical pretreatment combined with high intensity

ultrasonication followed by freeze-drying. Microstructure observations demonstrate that the ultralong CNFs were organized by millions of parallel nanofibrils 1–5 nm in width and several microns long; these produce almost transparent and highly viscous dispersion. The main composition of the CNFs was cellulose due to the removal of non-cellulosic polysaccharides via chemical treatment. Crystallinity and thermal stability increased with the removal of matrix components. The crystallinity of the CNFs reached approximately 61.25%, whereas the thermal degradation temperature of the CNFs was over 309 °C. The present work has also been fabricated millimeter-long CNFs from wheat straw and softwood fibers, and we hope that the method described here could be extended to provide a route to produce ultralong nanofibers from other natural polysaccharide materials.

Acknowledgements

This work was financially supported by the Fundamental Research Funds for the Central Universities (DL09EB01-3). This work was also supported by the Program for New Century Excellent Talents in University.

Appendix A. Supplementary data

Supplementary data associated with this article can be found, in the online version, at doi:10.1016/j.carbpol.2011.04.061.

References

Abe, K., Iwamoto, S., & Yano, H. (2007). Obtaining cellulose nanofibers with a uniform width of 15 nm from wood. *Biomacromolecules*, *8*(10), 3276–3278.
Abe, K., & Yano, H. (2009). Comparison of the characteristics of cellulose microfibril aggregates of wood, rice straw and potato tuber. *Cellulose*, *16*(6), 1017–1023.
Abe, K., & Yano, H. (2010). Comparison of the characteristics of cellulose microfibril aggregates isolated from fiber and parenchyma cells of Moso bamboo (Phyllostachys pubescens). *Cellulose*, *17*(2), 271–277.
Alemdar, A., & Sain, M. (2008). Isolation and characterization of nanofibers from agricultural residues – Wheat straw and soy hulls. *Bioresource Technology*, *99*(6), 1664–1671.
Araki, J., Wada, M., Kuga, S., & Okano, T. (1998). Flow properties of microcrystalline cellulose suspension prepared by acid treatment of native cellulose. *Colloids and Surfaces A: Physicochemical and Engineering Aspects*, *142*(1), 75–82.
Azizi Samir, M. A. S., Alloin, F., & Dufresne, A. (2005). Review of recent research into cellulosic whiskers. Their properties and their application in nanocomposite field. *Biomacromolecules*, *6*(2), 612–626.
Beck-Candanedo, S., Roman, M., & Gray, D. G. (2005). Effect of reaction conditions on the properties and behavior of wood cellulose nanocrystal suspensions. *Biomacromolecules*, *6*(2), 1048–1054.
Beecher, J. F. (2007). Organic materials: Wood, trees and nanotechnology. *Nature Nanotechnology*, *2*(8), 466–467.
Bergenstråhle, M., Berglund, L. A., & Mazeau, K. (2007). Thermal response in crystalline Iβ cellulose: A molecular dynamics study. *The Journal of Physical Chemistry B*, *111*(30), 9138–9145.
Berglund, L. A. (2005). Natural fibers. In A. K. Mohanty, M. Misra, & L. T. Drzal (Eds.), *Biopolymers and their biocomposites* (pp. 807–832). Boca Raton, FL: CRC Press.
Burgess, J. (1979). Cellulose microfibrils – An end in sight? *Nature*, *278*(5701), 212.
Capadona, J. R., Van Den Berg, O., Capadona, L. A., Schroeter, M., Rowan, S. J., Tyler, D. J., et al. (2007). A versatile approach for the processing of polymer nanocomposites with self-assembled nanofibre templates. *Nature Nanotechnology*, *2*(12), 765–769.
Chakraborty, A., Sain, M., & Kortschot, M. (2005). Cellulose microfibrils: A novel method of preparation using high shear refining and cryocrushing. *Holzforschung*, *59*(1), 102–107.
Chakraborty, A., Sain, M., & Kortschot, M. (2006). Reinforcing potential of wood pulp-derived microfibres in a PVA matrix. *Holzforschung*, *60*(1), 53–58.
Chen, W., Yu, H., Liu, Y., Chen, P., Zhang, M., & Hai, Y. (2011). Individualization of cellulose nanofibers from wood using high-intensity ultrasonication combined with chemical pretreatments. *Carbohydrate Polymers*, *83*(4), 1804–1811.
Cheng, Q., Wang, S., Rials, T., & Lee, S. (2007). Physical and mechanical properties of polyvinyl alcohol and polypropylene composite materials reinforced with fibril aggregates isolated from regenerated cellulose fibers. *Cellulose*, *14*(6), 593–602.
Cheng, Q., Wang, S., & Rials, T. G. (2009). Poly(vinyl alcohol) nanocomposites reinforced with cellulose fibrils isolated by high intensity ultrasonication. *Composites Part A: Applied Science and Manufacturing*, *40*(2), 218–224.
Dong, S., & Roman, M. (2007). Fluorescently labeled cellulose nanocrystals for bioimaging applications. *Journal of the American Chemical Society*, *129*(45), 13810–13811.
Eichhorn, S., Dufresne, A., Aranguren, M., Marcovich, N., Capadona, J., Rowan, S., et al. (2010). Review: Current international research into cellulose nanofibres and nanocomposites. *Journal of Materials Science*, *45*(1), 1–33.
Elazzouzi-Hafraoui, S., Nishiyama, Y., Putaux, J.-L., Heux, L., Dubreuil, F., & Rochas, C. (2007). The shape and size distribution of crystalline nanoparticles prepared by acid hydrolysis of native cellulose. *Biomacromolecules*, *9*(1), 57–65.
Fan, Y., Saito, T., & Isogai, A. (2008). Preparation of chitin nanofibers from squid pen β-chitin by simple mechanical treatment under acid conditions. *Biomacromolecules*, *9*(7), 1919–1923.
Fukuzumi, H., Saito, T., Iwata, T., Kumamoto, Y., & Isogai, A. (2009). Transparent and high gas barrier films of cellulose nanofibers prepared by TEMPO-mediated oxidation. *Biomacromolecules*, *10*(1), 162–165.
Habibi, Y., Lucia, L. A., & Rojas, O. J. (2010). Cellulose nanocrystals: Chemistry, self-assembly, and applications. *Chemical Reviews*, *110*(6), 3479–3500.
Herrick, F. W., Casebier, R. L., & Hamilton, J. K. (1983). Microfibrillated cellulose: Morphology and accessibility. *Journal of Applied Polymer Science: Applied Polymer Symposium*, *37*, 797–813.
Henriksson, M., Henriksson, G., Berglund, L., & Lindstrom, T. (2007). An environmentally friendly method for enzyme-assisted preparation of microfibrillated cellulose (MFC) nanofibers. *European Polymer Journal*, *43*(8), 3434–3441.
Ifuku, S., Nogi, M., Abe, K., Yoshioka, M., Morimoto, M., Saimoto, H., et al. (2009). Preparation of chitin nanofibers with a uniform width as α-chitin from crab shells. *Biomacromolecules*, *10*(6), 1584–1588.
Isogai, A., Saito, T., & Fukuzumi, H. (2011). TEMPO-oxidized cellulose nanofibers. *Nanoscale*, *3*(1), 71–85.
Iwamoto, S., Abe, K., & Yano, H. (2008). The effect of hemicelluloses on wood pulp nanofibrillation and nanofiber network characteristics. *Biomacromolecules*, *9*, 1022–1026.
Kim, C.-W., Kim, D.-S., Kang, S.-Y., Marquez, M., & Joo, Y. L. (2006). Structural studies of electrospun cellulose nanofibers. *Polymer*, *47*(14), 5097–5107.
Klemm, D., Heublein, B., Fink, H.-P., & Bohn, A. (2005). Cellulose: Fascinating biopolymer and sustainable raw material. *Angewandte Chemie International Edition*, *44*(22), 3358–3393.
Li, D., & Xia, Y. (2004). Electrospinning of nanofibers: Reinventing the wheel? *Advanced Materials*, *16*(14), 1151–1170.
Li, Q., & Renneckar, S. (2011). Supramolecular structure characterization of molecularly thin cellulose I nanoparticles. *Biomacromolecules*, *12*(3), 650–659.
Marchessault, R. H., Morehead, F. F., & Walter, N. M. (1959). Liquid crystal systems from fibrillar polysaccharides. *Nature*, *184*(4686), 632–633.
Nishino, T., Matsuda, I., & Hirao, K. (2004). All-cellulose composite. *Macromolecules*, *37*(20), 7683–7687.
Nishiyama, Y., Langan, P., & Chanzy, H. (2002). Crystal structure and hydrogen-bonding system in cellulose Iβ from synchrotron X-ray and neutron fiber diffraction. *Journal of the American Chemical Society*, *124*(31), 9074–9082.
Nishiyama, Y., Sugiyama, J., Chanzy, H., & Langan, P. (2003). Crystal structure and hydrogen bonding system in cellulose Iα from synchrotron X-ray and neutron fiber diffraction. *Journal of the American Chemical Society*, *125*(47), 14300–14306.
Nogi, M., Iwamoto, S., Nakagaito, A. N., & Yano, H. (2009). Optically transparent nanofiber paper. *Advanced Materials*, *21*(16), 1595–1598.
Pääkkö, M., Ankerfors, M., Kosonen, H., Nykänen, A., Ahola, S., Österberg, M., et al. (2007). Enzymatic hydrolysis combined with mechanical shearing and high-pressure homogenization for nanoscale cellulose fibrils and strong gels. *Biomacromolecules*, *8*(6), 1934–1941.
Pääkkö, M., Vapaavuori, J., Silvennoinen, R., Kosonen, H., Ankerfors, M., Lindstrom, T., et al. (2008). Long and entangled native cellulose I nanofibers allow flexible aerogels and hierarchically porous templates for functionalities. *Soft Matter*, *4*(12), 2492–2499.
Saito, T., Kimura, S., Nishiyama, Y., & Isogai, A. (2007). Cellulose nanofibers prepared by TEMPO-mediated oxidation of native cellulose. *Biomacromolecules*, *8*(8), 2485–2491.
Sakurada, I., Nukushina, Y., & Ito, T. (1962). Experimental determination of the elastic modulus of crystalline regions in oriented polymers. *Journal of Polymer Science*, *57*(165), 651–660.
Segal, L., Creely, J. J., Martin, A. E., Jr., & Conrad, C. M. (1959). An empirical method for estimating the degree of crystallinity of native cellulose using the X-ray diffreactometer. *Textile Research Journal*, *29*, 786–794.
Sehaqui, H., Liu, A., Zhou, Q., & Berglund, L. A. (2010). Fast preparation procedure for large. Flat cellulose and cellulose/inorganic nanopaper structures. *Biomacromolecules*, *11*(9), 2195–2198.
Shopsowitz, K. E., Qi, H., Hamad, W. Y., & MacLachlan, M. J. (2010). Free-standing mesoporous silica films with tunable chiral nematic structures. *Nature*, *468*(7322), 422–425.
Siqueira, G., Bras, J., & Dufresne, A. (2008). Cellulose whiskers versus microfibrils: Influence of the nature of the nanoparticle and its surface functionalization on the thermal and mechanical properties of nanocomposites. *Biomacromolecules*, *10*(2), 425–432.
Siró, I., & Plackett, D. (2010). Microfibrillated cellulose and new nanocomposite materials: A review. *Cellulose*, *17*(3), 459–494.
Somerville, C., Bauer, S., Brininstool, G., Facette, M., Hamann, T., Milne, J., et al. (2004). Toward a systems approach to understanding plant cell walls. *Science*, *306*(5705), 2206–2211.
Svagan, A. J., Samir, M. A. S. A., & Berglund, L. A. (2008). Biomimetic foams of high mechanical performance based on nanostructured cell walls reinforced by native cellulose nanofibrils. *Advanced Materials*, *20*(7), 1263–1269.

Tischer, P. C. S. F., Sierakowski, M. R., Westfahl, H., & Tischer, C. A. (2010). Nanostructural reorganization of bacterial cellulose by ultrasonic treatment. *Biomacromolecules*, *11*(5), 1217–1224.

Turbak, A. F., Snyder, F. W., & Sandberg, K. R. (1983). Microfibrillated cellulose, a new cellulose product: Properties, uses, and commercial potential. *Journal of Applied Polymer Science: Applied Polymer Symposium*, *37*, 815–827.

Uetani, K, & Yano, H. (2011). Nanofibrillation of wood pulp using a high-speed blender. *Biomacromolecules*, *12*(2), 348–353.

Xia, Y. (2008). Nanomaterials at work in biomedical research. *Nature Materials*, *7*(10), 758–760.

Xie, J., Li, X., & Xia, Y. (2008). Putting electrospun nanofibers to work for biomedical research. *Macromolecular Rapid Communications*, *29*(22), 1775–1792.

Zhao, H., Feng, X., & Gao, H. (2007). Ultrasonic technique for extracting nanofibers from nature materials. *Applied Physics Letters*, *90*, 073112.